J|A|C|S ARTICLES

Published on Web 01/20/2009

Orthogonal "Relay" Reactions for Designing Functionalized Soft Nanoparticles

Hamilton Kakwere and Sébastien Perrier*

Key Centre for Polymers & Colloids, School of Chemistry, University of Sydney, Sydney, NSW 2006, Australia

Received September 23, 2008; E-mail: s.perrier@chem.usyd.edu.au

Abstract: The combination of reversible addition−fragmentation chain transfer (RAFT) chemistry followed by thiol-based "click" chemistry, known as an orthogonal "relay" reaction as one step complements the other, was used to produce surface-functionalized soft nanoparticles. Thiocarbonyl thio compounds were first used in the presence of vinyl monomers and a source of radicals to control the growth of the polymeric chains (via the RAFT process) and then reduced to thiols and utilized as a handle for functionalization of the resulting polymer chain ends (via a thiol-based click reaction). Both reactions occur under mild conditions and offer excellent control over the properties of the final product, and the thiol addition shows all the benefits of a click reaction, without requiring the use of a catalyst. This simple chemistry opens up the route to the production of a wide range of functional materials, and the concept is illustrated by the formation of nanoparticle-based gels, fluorescent-tagged particles, and protein−nanoparticle conjugates.

Introduction

Nanostructured materials of well-defined design are attracting considerable interest because of the variety of their applications. Nanoparticles are a class of such materials, which have been extensively developed in recent years and are now finding applications in chemistry, medicine, material science, and so on. With the advance of modern synthetic techniques,[1] the synthesis of functionalized organic nanoparticles has generated wide interest over recent years, as a result of the vast range of possible applications of these types of materials, including targeted drug delivery, surface coatings, nanoreactors, and stabilization of emulsions.[2] Arguably the most versatile and widely employed route to these types of nanomaterials is through the synthesis of amphiphilic block copolymers, which consist of at least one hydrophilic segment attached to at least one hydrophobic segment to form a linear polymeric chain. When added to water at concentrations higher than the critical micelle concentration (cmc), these polymeric structures are capable of self-organizing via noncovalent interactions in a uniform manner (i.e., self-assembling) to give different types of nanometer-sized supramolecular structures (e.g., spheres, vesicles, cylinders, etc.) depending on the chemical composition of the copolymer and its environment.[3] This free-energy-driven self-assembly is based on the phase separation of the insoluble blocks, which is restricted to the nanometric scale by a surrounding shell of soluble blocks. The use of polymeric amphiphiles permits control of the particle size by adjustment of the block copolymer chain length, and polymer micelles are more stable and have lower cmc's than small-molecule surfactant micelles. The aggregate structures formed by self-assembly of block copolymers are, however, not very robust with respect to changes in their surroundings. Their intrinsic structure, based on dynamic self-assembly of amphiphiles, makes the micelles susceptible to disintegration upon variation of the conditions in their environment (e.g., pH, temperature, ionic strength), thereby limiting their applicability, especially in drug delivery.[3] An elegant route toward the stabilization of micellar structure is the cross-linking of the core[4] or the shell[5] of the micelles. Of these two approaches, the production of shell cross-linked micelles (SCMs) is considered as the more versatile route, as it allows for greater core mobility, encapsulation, and surface binding ability of the nanostructures.[5]

The recent advances in living radical polymerization techniques[6] give access to a wider range of nanoparticles by adding flexibility, diversity, and functionality in the design of block copolymers. Nitroxide-mediated polymerization (NMP), atom-transfer radical polymerization (ATRP), and reversible addition−fragmentation chain transfer (RAFT) polymerization are all techniques that have been employed to produce well-defined

(1) Hawker, C. J.; Wooley, K. L. *Science* **2005**, *309*, 1200.
(2) (a) Bosman, A. W.; Vestberg, R.; Heumann, A.; Fréchet, J. M. J.; Hawker, C. J. *J. Am. Chem. Soc.* **2003**, *125*, 715. (b) Butun, V.; Lowe, A. B.; Billingham, N. C.; Armes, S. P. *J. Am. Chem. Soc.* **1999**, *121*, 4288. (c) Cheng, C.; Qi, K.; Germack, D. S.; Khoshdel, E.; Wooley, K. L. *Adv. Mater.* **2007**, *19*, 2830. (d) Hoeben, F. J. M.; Jonkheijm, P.; Meijer, E. W.; Schenning, A. P. H. J. *Chem. Rev.* **2005**, *105*, 1491. (e) Kang, Y.; Taton, T. A. *Angew. Chem., Int. Ed.* **2005**, *44*, 409. (f) Li, Z.; Kesselman, E.; Talmon, Y.; Hillmyer, M. A.; Lodge, T. P. *Science* **2004**, *306*, 98. (g) Pochan, D. J.; Chen, Z.; Cui, H.; Hales, K.; Qi, K.; Wooley, K. L. *Science* **2004**, *306*, 94. (h) Vriezema, D. M.; Aragones, M. C.; Elemans, J. A. A. W.; Cornelissen, J. J. L. M.; Rowan, A. E.; Nolte, R. J. M. *Chem. Rev.* **2005**, *105*, 1445.
(3) (a) O'Reilly, R. K.; Hawker, C. J.; Wooley, K. L. *Chem. Soc. Rev.* **2006**, *35*, 1068. (b) Read, E. S.; Armes, S. P. *Chem. Commun.* **2007**, 3021. (c) Stenzel, M. H. *Chem. Commun.* **2008**, 3486.
(4) Guo, A.; Liu, G.; Tao, J. *Macromolecules* **1996**, *29*, 2487.
(5) Thurmond, K. B.; Kowalewski, T.; Wooley, K. L. *J. Am. Chem. Soc.* **1996**, *118*, 7239.
(6) *Controlled/Living Radical Polymerization: from Synthesis to Materials*; Matyjaszewski, K., Ed.; American Chemical Society: Washington, DC, 2006.

10.1021/ja8075499 CCC: $40.75

amphiphilic block copolymers. The robustness of these free-radical processes permits the introduction of reactive groups, either in the backbone of the block forming the shell of the micelle or at the chain ends; these groups can react with each other under given conditions (e.g., UV light) or can be reacted with difunctional small molecules to create cross-linking. To further widen the scope of applications, surface functionalization of shell cross-linked nanoparticles has been employed to introduce several types of specific active groups at the surface of the shell. Numerous functionalities have been attached to shell cross-linked nanoparticles, such as sugar,[7] folic acid,[8] cancer-cell-targeting ligands,[9] proteins,[10,11] and oligonucleic acids.[12,13] Syntheses of cross-linked nanoparticles labeled with peptides,[14] antigens,[15] fluorescent dye molecules,[16] and biotin[17] have also been reported. Several approaches to the synthesis of surface-functionalized cross-linked nanoparticles have been established over the years, most being *pre*-micelle-formation methods involving the functionalization of the chain end of the hydrophilic block. However, this approach suffers from many drawbacks: (i) the procedure does not allow good control over the availability of the functionality at the surface of the particle, since the functional group can be buried within the shell as a result of the molecular weight distribution of the polymeric chains and the various conformations they may adopt when assembled; (ii) the synthesis of the polymers is limited by the potential side reactions with the chain-end functionality, depending of the polymerization technique adopted; and (iii) each type of functional particle requires the synthesis of a specific polymer, followed by its self-assembly. On the other hand, *post*-micelle-formation functionalization has clear benefits, as it allows for flexibility in the introduction of functional groups onto the nanoparticles, permits an increase in the range of possible functional groups, and maximizes their availability at the surface of the particles. Surprisingly, despite the great potential of the approach, there are very few examples of post-formation functionalization of cross-linked micelles. O'Reilly and co-workers[16,18] used NMP and RAFT polymerization to make amphiphilic block copolymers with azide end functionalities, which were micellized and then stabilized via cross-linking. The azide-functionalized nanoparticles were fluorescently tagged by copper-catalyzed azide−alkyne cycloaddition (a "click" reaction[19]) using an alkynyl-functionalized dye. These methods have proved to be powerful and very versatile, but a closer look at the protocols employed shows that they are rather complicated and lengthy, involving many steps of protection and deprotection chemistry in the presence of catalysts. In view of these drawbacks, research on finding shorter, more versatile, and simpler approaches is thus warranted. Recently, Wooley and co-workers[20] reported a much simpler route to surface-functionalized nanoparticles involving the use of RAFT polymerization to obtain *N*-acryloxysuccinimide (NAS)-containing block copolymers, which were self-assembled and then simultaneously cross-linked and functionalized via the NAS units using a diamine cross-linker and an amine-functionalized fluorescent tag. In another recent publication, block copolymers with halide end groups were synthesized and transformed into shell cross-linked nanoparticles having their surfaces decorated with halide end groups, from which functionalization was undertaken by ATRP of dimethylaminoethyl methacrylate, thus making the nanoparticles stimuli-responsive.[21] The key synthetic approach in these studies is the use of orthogonal click reactions, which are robust and give access to a range of functionalities under relatively mild reaction conditions. However, in most cases, such reactions require the use of specifically designed reagents and catalysts.[19]

We present here the production of universally surface-functionalized polymeric nanoparticles by exploitation of the ubiquity of a reagent that can control both polymer synthesis and postpolymerization functionalization, a route that could be described as an orthogonal "relay" reaction. Our synthetic approach is based on thiocarbonyl thio reactive groups, which, in the presence of vinyl monomers and a source of radicals, control the growth of the polymeric chains by end-capping them to yield chains of predictable lengths (via the RAFT process[22,23]) and then can be reduced into a thiol and utilized as a handle for functionalization of the resulting polymer chain ends (via a click reaction). Both reactions occur under mild conditions and offer excellent control over the properties of the final product, and the thiol reaction shows all the benefits of a click reaction. The key aspects of this approach are that (1) the polymerization mediator (the thiocarbonyl thio moiety) also behaves as a protecting group for the thiol functionality and can be easily removed and (2) the resulting thiol can be used for a click reaction that does not require a catalyst and is undertaken under very mild conditions (e.g., room temperature). Recently, Nystrom and Wooley[11] reported the synthesis of thiol-functionalized knedel-like nanoparticles, where the thiol functionality was introduced into the hydrophilic shell of the particles via a complex multistep procedure. In our approach, the procedure is greatly simplified, as the thiocarbonyl thio end groups of amphiphilic block copolymers synthesized via RAFT can easily be converted into thiols by reduction.[22,23] The thiol functionality is an extremely versatile handle for introducing functionalization, as it is capable of reacting in quantitative yields under mild reaction conditions with other thiols,[24,25] gold,[26] maleimides,[27−33]

(7) Joralemon, M. J.; Murthy, K. S.; Remsen, E. E.; Becker, M. L.; Wooley, K. L. *Biomacromolecules* **2004**, *5*, 903.
(8) Pan, D.; Turner, J. L.; Wooley, K. L. *Chem. Commun.* **2003**, 2400.
(9) Pan, D. J.; Turner, J. L.; Wooley, K. L. *Macromolecules* **2004**, *37*, 7109.
(10) Liu, H.; Jiang, X.; Fan, J.; Wang, G.; Liu, S. *Macromolecules* **2007**, *40*, 9074.
(11) Nystrom, A. M.; Wooley, K. L. *Tetrahedron* **2008**, *64*, 8543.
(12) Turner, J. L.; Becker, M. L.; Li, X. X.; Taylor, J. S. A.; Wooley, K. L. *Soft Matter* **2005**, *1*, 69.
(13) Zhang, L.; Nguyen, T. L. U.; Bernard, J.; Davis, T. P.; Barner-Kowollik, C.; Stenzel, M. H. *Biomacromolecules* **2007**, *8*, 2890.
(14) Becker, M. L.; Liu, J. Q.; Wooley, K. L. *Biomacromolecules* **2005**, *6*, 220.
(15) Joralemon, M. J.; Smith, N. L.; Holowka, D.; Baird, B.; Wooley, K. L. *Bioconjugate Chem.* **2005**, *16*, 1246.
(16) O'Reilly, R. K.; Joralemon, M. J.; Wooley, K. L.; Hawker, C. J. *Chem. Mater.* **2005**, *17*, 5976.
(17) Qi, K.; Ma, Q.; Remsen, E. E.; Clark, C. G.; Wooley, K. L. *J. Am. Chem. Soc.* **2004**, *126*, 6599.
(18) O'Reilly, R. K.; Joralemon, M. J.; Hawker, C. J.; Wooley, K. L. *J. Polym. Sci., Part A: Polym. Chem.* **2006**, *44*, 5203.
(19) Kolb, H. C.; Finn, M. G.; Sharpless, K. B. *Angew. Chem., Int. Ed.* **2001**, *40*, 2004.
(20) Li, Y.; Akiba, I.; Harrisson, S.; Wooley, K. L. *Adv. Funct. Mater.* **2008**, *18*, 551.
(21) Babin, J.; Lepage, M.; Zhao, Y. *Macromolecules* **2008**, *41*, 1246.
(22) Moad, G.; Rizzardo, E.; Thang, S. H. *Aust. J. Chem.* **2006**, *59*, 669.
(23) Perrier, S.; Takolpuckdee, P. *J. Polym. Sci., Part A: Polym. Chem.* **2005**, *43*, 5347.
(24) York, A. W.; Kirkland, S. E.; McCormick, C. L. *Adv. Drug Delivery. Rev.* **2008**, *60*, 1018.
(25) Kim, Y.; Ho, S. O.; Gassman, N. R.; Korlann, Y.; Landorf, E. V.; Collart, F. R.; Weiss, S. *Bioconjugate Chem.* **2008**, *19*, 786.
(26) Xu, H.; Xu, J.; Jiang, X.; Zhu, Z.; Rao, J.; Yin, J.; Wu, T.; Liu, H.; Liu, S. *Chem. Mater.* **2007**, *19*, 2489.
(27) Scales, C. W.; Convertine, A. J.; McCormick, C. L. *Biomacromolecules* **2006**, *7*, 1389.

iodoacetamides,[34] alkenes,[35,36] and acrylates (via Michael addition);[37,38] this versatility was exploited by Hawker and co-workers[35] and Dondoni,[36] who demonstrated that the free-radical reactions of thiols with enes have all the attributes of a click reaction. We demonstrate how the resulting thiol-decorated nanoparticles can easily be functionalized by conjugating them to a fluorescent tag or a protein and by using the thiol groups as cross-linkers to produce novel gels. The resulting structures are comparable to natural viral architectures, as both structures possess self-assembled shells and similar scales and are capable of selective targeting.

Results and Discussion

Amphiphilic block copolymers of ethyl acrylate (EA) and hydroxyethylacrylate (HEA)-*co*-NAS were synthesized via 2-ethylsulfanylthiocarbonylsulfanylpropionic acid ethyl ester (ETSPE)[39,40]-mediated RAFT polymerization. EA was selected for building the hydrophobic segment, and HEA was chosen as hydrophilic monomer. NAS was introduced in the hydrophilic block to facilitate the cross-linking of the micelle shell. ETSPE is an excellent chain-transfer agent for controlling the living polymerization of acrylates, and the use of acrylate derivatives to generate the hydrophilic and hydrophobic blocks of the amphiphilic block copolymer allows for precise control over chain lengths and the molecular weight distribution.[22,23] The random copolymerization of NAS with comonomers (e.g., acryloylmorpholine[20] or dimethyl acrylamide[41]) via RAFT has also been shown to yield copolymers of well-controlled molecular weight. Polymerization of EA was first undertaken to yield a polymer having a number-average molecular weight (M_n) of 23 000 g/mol and a polydispersity index (PDI) of 1.10. The poly(EA) [P(EA)] was chain-extended in the presence of HEA with varying amounts of NAS, yielding the block copolymers P[EA_{117}-*b*-(HEA_{92}-*co*-NAS_9)] and P[EA_{117}-*b*-(HEA_{85}-*co*-NAS_{16})].

The P[EA-*b*-(HEA-*co*-NAS)] block copolymers were initially dissolved in methanol, a solvent that solubilizes both the hydrophilic and hydrophobic blocks; this was followed by slow addition of water, a nonsolvent for the P(EA) block, to encourage micellization. The resulting micelle solutions were analyzed by dynamic light scattering (DLS) and transmission electron microscopy (TEM) (Table 1). Particle size analysis by DLS gave monomodal symmetrical distributions with low polydispersities (<0.1), indicating that the sizes of the micelles were nearly uniform with average micelle diameters of 39 nm for P[EA_{117}-*b*-(HEA_{92}-*co*-NAS_9)] and 59 nm for P[EA_{117}-*b*-(HEA_{85}-*co*-NAS_{16})]. The increase in the size of the micelles, despite keeping the overall degrees of polymerization (DP's) constant, is related to the increase in concentration of NAS in the hydrophilic block. Indeed, NAS undergoes hydrolysis in water during the formation of the micelles, yielding *N*-hydroxysuccinimide and a carboxylic acid group that is pendant from the polymeric chain (see Figure S1 in the Supporting Information).[41] Carboxylic acid groups are more polar than hydroxyl groups (from HEA), thus improving hydration of the shells of the micelles by water.[42,43] Furthermore, the carboxylic acid groups formed on the polymeric chains are charged at the pH of the aqueous solution (pH ~7), thus resulting in increased repulsive forces between the chains, which would increase with an increasing number of NAS units. The particles were also analyzed by TEM, and smaller diameters were observed (Figure 1). The discrepancy between the DLS and TEM analyses is due to the fact that the micelles are fully hydrated in solution during the DLS measurement but dried under TEM conditions.[42,44] The difference in the sizes obtained from the DLS and TEM analyses is more significant for the particles incorporating a higher concentration in NAS (entry 2, Table 1), thus confirming the effect of the hydrolyzed NAS on the solvatation of the micelle shell. It is also noteworthy that the low glass transition temperature ($T_g = -20$ °C) of the P(EA) block causes the micelles to slightly lose their spherical shape in their dry state.

Table 1. Average Diameters of P[EA-*b*-(HEA-*co*-NAS)] Micelle Solutions in Water before (Micelles) and after (SCM) Crosslinking with HMDA

	micelles (nm)		SCM (nm)	
polymer	TEM	DLS	TEM	DLS
P[EA_{117}-*b*-(HEA_{92}-*co*-NAS_9)]	34 ± 3	39 ± 1 (99%)	30 ± 2	42 ± 1 (90%)
P[EA_{117}-*b*-(HEA_{85}-*co*-NAS_{16})]	38 ± 7	59 ± 1 (99%)	28 ± 3	61 ± 1 (99%)

A variety of techniques for cross-linking the shells of polymeric micelles have been reported. Existing strategies include radical chemistry, carbodiimide coupling, UV-induced coupling, Michael addition, quaternization, esterification, copper-catalyzed azide−alkyne cycloaddition, disulfide/thiol chemistry, and polyelectrolyte complexation.[3]We opted for the chemistry developed by McCormick and co-workers,[41] who reported the facile cross-linking of micelle shells via reaction of succinimide groups with ethylenediamine. Cross-linking reactions were carried out in the presence of hexamethylenediamine (HMDA) in dilute aqueous solutions with micellar concentrations of 0.75 mg/mL to avoid intermicellar cross-linking.[45] Before the cross-linking reactions, the pH of micellar solutions was adjusted to ~9 with a phosphate buffer to prevent the protonation of HMDA at low pH values ($pK_a \geq 10$). McCormick and co-workers[41] have shown that although the succinimide group can be

(28) Kullman, J. P.; Yu, T.; Chen, X. H.; Neal, R.; Ercal, N.; Armstrong, D. W. *J. Liq. Chromatogr. Relat. Technol.* **2000**, *23*, 1941.
(29) Kulkarni, S.; Schilli, C.; Grin, B.; Muller, A. H. E.; Hoffman, A. S.; Stayton, P. S. *Biomacromolecules* **2006**, *7*, 2736.
(30) Chen, Y.; Thakar, R.; Snee, P. T. *J. Am. Chem. Soc.* **2008**, *130*, 3744.
(31) Mantovani, G.; Lecolley, F.; Tao, L.; Haddleton, D. M.; Clerx, J.; Cornelissen, J. J. L. M.; Velonia, K. *J. Am. Chem. Soc.* **2005**, *127*, 2966.
(32) Tolstyka, Z. P.; Kopping, J. T.; Maynard, H. A. *Macromolecules* **2008**, *41*, 599.
(33) Pounder, R. J.; Sanford, M. J.; Brooks, P.; Richards, S. J.; Dove, A. P. *Chem. Commun.* **2008**, 5158.
(34) Toutchkine, A.; Nalbant, P.; Hahn, K. M. *Bioconjugate Chem.* **2002**, *13*, 387.
(35) Killops, K. L.; Campos, L. M.; Hawker, C. J. *J. Am. Chem. Soc.* **2008**, *130*, 5062.
(36) Dondoni, A. *Angew. Chem., Int. Ed.* **2008**, *47*, 2.
(37) Cellesi, F.; Tirelli, N.; Hubbell, J. A. *Macromol. Chem. Phys.* **2002**, *203*, 1466.
(38) Lee, B. H.; West, B.; McLemore, R.; Pauken, C.; Vernon, B. L. *Biomacromolecules* **2006**, *7*, 2059.
(39) Wood, M. R.; Duncalf, D. J.; Rannard, S. P.; Perrier, S. *Org. Lett.* **2006**, *8*, 553.
(40) Wood, M. R.; Duncalf, D. J.; Findlay, P.; Rannard, S. P.; Perrier, S. *Aust. J. Chem.* **2007**, *60*, 772.
(41) Li, Y.; Lokitz, B. S.; McCormick, C. L. *Macromolecules* **2006**, *39*, 81.
(42) Terreau, O.; Luo, L. B.; Eisenberg, A. *Langmuir* **2003**, *19*, 5601.
(43) Gao, L.; Shi, L.; Zhang, W.; An, Y.; Jiang, X. *Macromol. Chem. Phys.* **2006**, *207*, 521.
(44) Madsen, J.; Armes, S. P.; Bertal, K.; Lomas, H.; MacNeil, S.; Lewis, A. L. *Biomacromolecules* **2008**, *9*, 2265.
(45) Bütün, V.; Wang, X.-S.; de Paz Báñez, M. V.; Robinson, K. L.; Billingham, N. C.; Armes, S. P.; Tuzar, Z. *Macromolecules* **2000**, *33*, 1.

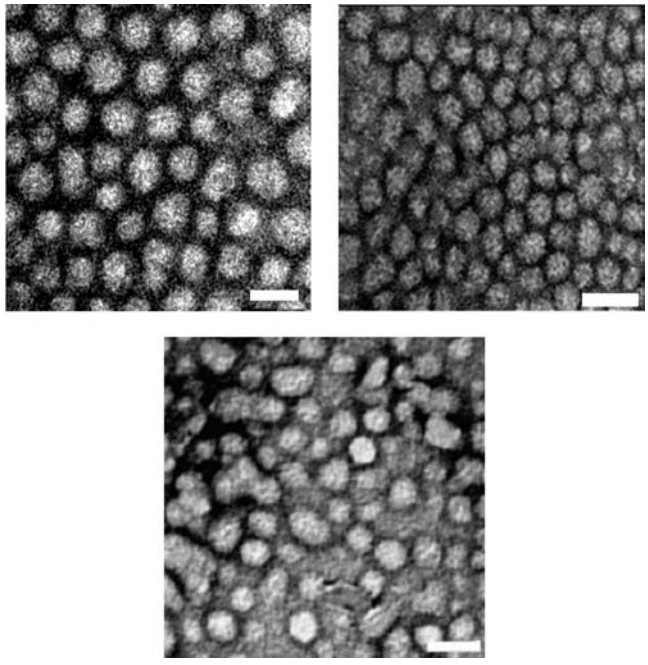

Figure 1. TEM images of micelle solutions of P[EA_{117}-*b*-(HEA_{85}-*co*-NAS_{16})] (top left) before and (top right) after cross-linking with HMDA and (bottom) after cross-linking and dissolution in DMF. Scale bar is 50 nm. The corresponding images of P[EA_{117}-*b*-(HEA_{92}-*co*-NAS_9)] are shown in Figure S3 in the Supporting Information.

hydrolyzed in water, a significant number of reactive units still remain even after prolonged exposure. Indeed, we obtained 85% cross-linking of the NAS unit, as estimated by ^{1}H NMR (see Figure S2 in the Supporting Information). DLS analyses revealed a single population of particles having sizes close to that of the micelles prior to cross-linking (Table 1), thus demonstrating that intermicellar cross-linking did not occur.[5] TEM analyses confirmed the presence of a single population of particles, with average sizes smaller than that measured by DLS for the reasons discussed above (Figure 1).

In order to assess the success of the cross-linking reaction and the stability of the SCMs, solutions of micelles before and after cross-linking were subjected to freeze-drying. A yellow-colored powder (due to the presence of the trithiocarbonate end group of the block copolymers) was recovered in both cases and fully dissolved upon addition of DMF (a good solvent for both the hydrophilic and hydrophobic segments of the block copolymer). DLS measurements were then undertaken on the DMF solutions to verify the structures of the two families of aggregates. DLS revealed very small structures (<10 nm) in the DMF solution formed from the freeze-dried aqueous micelle solution, representing the block copolymers in their unimer forms, thus confirming that the micelles cannot hold their structure. On the other hand, DLS analysis of the DMF solution of the SCMs revealed that the particles had kept their structure, although their sizes had significantly increased because the solvent swelled the nanoparticles. The swelling of the SCMs by a solvent is a very useful feature that can be exploited to load active agents into the cores of the nanoparticles.[46] Analyses of particles with different amounts of NAS {P[EA_{117}-*b*-(HEA_{92}-*co*-NAS_9)] and P[EA_{117}-*b*-(HEA_{85}-*co*-NAS_{16})]} revealed that an increase in the number of succinimide groups leads to smaller particles (133.1 and 116.0 nm, respectively), as the cross-linking density on the shell is increased, thus limiting the swelling of the structure. TEM images of the DMF-solubilized nanoparticles (Figure 1) confirm that the cross-linked nanostructures did not disintegrate in DMF. Furthermore, the sizes measured by TEM after dissolution of the particles in DMF are comparable to those observed by TEM from aqueous solution, confirming that the swelling is a solvent effect.

By synthesizing the amphiphilic block copolymers via RAFT by chain extension of the hydrophobic block with a hydrophilic segment, we positioned the thiocarbonyl thio group at the hydrophilic chain end of the polymer, with the aim of locating it at the surface of the shell of the SCM. The chemistry of reduction of thioesters into thiols is well-known, and a variety of reducing agents have been used on RAFT-synthesized polymers to produce polymers having thiols at their ω-chain ends.[22,23] Thiolation of the SCMs was undertaken by reduction of the thiocarbonyl thio RAFT end groups available on the surfaces of the stabilized nanoparticles using sodium borohydride in aqueous solution.[47] Conversion of the thiocarbonyl thio ω-chain end groups to thiols was confirmed by Raman spectroscopy, with the disappearance of the stretches at 1022 and 675 cm^{-1} [for C═S and C(S)−S, respectively] (see Figure S4 in the Supporting Information). The chemistry of thiols has been very well documented, especially in biology and biochemistry via, for instance, reactions at cysteine, a thiol-containing amino acid, to introduce conjugates or functional groups along the backbone of peptides and proteins.[48] Thiols are well-known to react rapidly and quantitatively with maleimides, acrylates, thiols (forming disulfide bridges), and alkenes. The selectivity, rapidity and high yields of such reactions have led them to be integrated into the family of click reactions.[33,35,36] The following describes three examples of the versatility of our novel functionalizable nanoparticles.

The most obvious and easiest modification of the thiol functionality is the formation of disulfide bridges. Following the reduction of the trithiocarbonate groups into thiols, the particles were placed in an oxidative environment, which triggers the formation of thiol−thiol coupling. Particle size measurements on solutions of the functionalized nanoparticles via DLS showed multiple peaks at larger diameters than those of the nonfunctionalized nanoparticles, due to particle aggregation arising from formation of disulfide bridges between the particles via dynamic thiol−thiol coupling (Figure 2). Under dilute conditions, a mixture of unimeric micelles and larger aggregates was observed, as the disulfide coupling occurs between thiols on the same particle as well as those on different particles. Increasing the concentration of the particles in solution favors intermicellar disulfide bridges, as illustrated by the disappearance of the signal from the single micelles; this yields larger aggregates, which eventually can form a gel. This behavior is fully reversible upon addition of a reducing agent such as tris(2-carboxyethyl)phosphine (TCEP), which re-forms unimeric micelles. Alternatively, a biologically relevant reducer such as glutathione, an oligopeptide containing a cysteine residue and used in nature to reduce disulfide bridges, has similar effects. This approach opens up the way to the formation of responsive hydrogels based on soft nanoparticles.

(46) Gaucher, G.; Dufresne, M. H.; Sant, V. P.; Kang, N.; Maysinger, D.; Leroux, J. C. *J. Controlled Release* **2005**, *109*, 169.
(47) Scales, C. W.; Convertine, A. J.; McCormick, C. L. *Biomacromolecules* **2006**, *7*, 1389.
(48) Roberts, M. J.; Bentley, M. D.; Harris, J. M. *Adv. Drug Delivery Rev.* **2002**, *54*, 459.

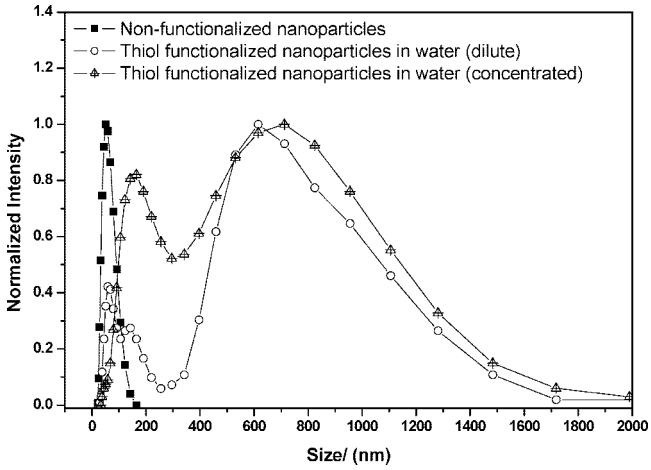

Figure 2. Particle size distributions of SCMs formed from P[EA_{117}-*b*-(HEA_{85}-*co*-NAS_{16})] in water before and after thiol functionalization in an oxidative environment.

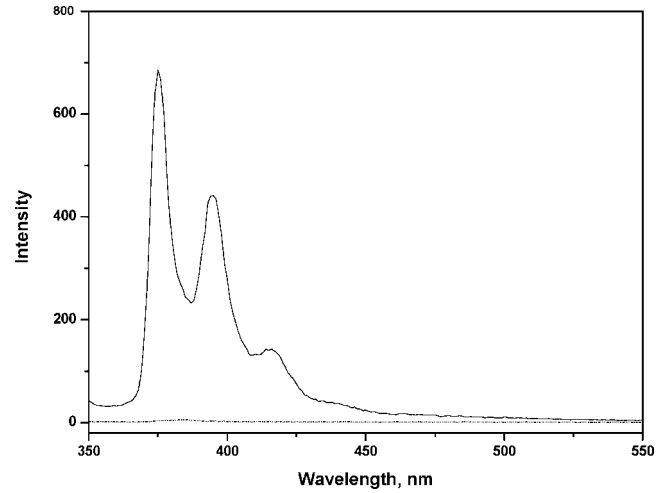

Figure 3. Emission spectra of functionalized cross-linked nanoparticles (dashed line) before and (solid line) after reaction with *N*-1-pyrenemaleimide.

Table 2. Amounts of Biotin Decorating the SCMs

sample	ΔA^b	C^c	R^d	$R_{theor}{}^e$
P[EA_{117}-*b*-(HEA_{85}-*co*-NAS_{16})]	0.088	0.028	9.8	41.15
P[EA_{117}-*b*-(HEA_{85}-*co*-NAS_{16})]^a	−0.001	0	0	0

[a] Functionalized cross-linked sample with no biotin attached. [b] Calculated change in absorbance, taking into account dilution of the HABA/avidin reagent by the sample. The theoretical amount of biotin is the amount of biotin expected if 100% of the thiol end groups had reacted; it was calculated on the basis of polymer molecular weight while also assuming that every polymer chain had a thiol end group. [c] Concentration of avidin (mmol/mL). [d] Concentration of avidin per gram of polymer. [e] Theoretical concentration of avidin per gram of polymer.

To demonstrate the reactivity of the nanoparticles in solution via their functionalized surfaces, we employed the well-known chemistry of thiol−maleimide coupling.[27−33] Thiol−maleimide coupling reactions are fast and selective and require mild reaction conditions. The thiol−maleimide coupling reactions were undertaken under a nitrogen atmosphere in the presence of TCEP in order to prevent the formation of disulfide bridges, which could significantly reduce the number of available reactive thiol groups. The reactions were performed under dry conditions to limit hydrolysis side reactions between water and maleimide[48] and in the presence of an excess of maleimide reagent because the reactive end groups were secondary thiols.[49] Reactions were performed in DMF, a high-dielectric-constant solvent, in the absence of a metal catalyst.[33] The thiol-functionalized nanoparticles were initially reacted with *N*-1-pyrenylmaleimide, which is nonfluorescent in aqueous solutions but becomes fluorescent when conjugated to thiols, with an excitation wavelength of 340 nm and an emission wavelength of 375 nm.[50] Figure 3 shows the fluorescence emission spectra of a typical sample before and after reaction with *N*-1-pyrenemaleimide, which demonstrate the success of the coupling, as typical emission spectra of thiol-conjugated *N*-1-pyrenemaleimide were observed.[51]

To exemplify further the versatility of the nanoparticles, their ability to react with a protein, avidin, was investigated. Avidin is formed from four subunits, each of which is able to bind one biotin molecule with a very high affinity (affinity constant $K_a = 10^{15}$ M). The avidin−biotin system has been studied as a model of protein−ligand interactions,[52] has led to a large number of applications, such as tumor pretargeting,[53] improved clinical diagnostics,[54] protein labeling, and proteomics, and is also used as a research tool in surface engineering, self-assembly studies, and drug delivery.[55] The particles were first reacted with biotin maleimide under the same conditions as described above. After dialysis, the biotinylated particles were put in the presence of a 4′-hydroxyazobenzene-2-carboxylic acid (HABA)−avidin complex. HABA and avidin form a weak complex in water ($K_d = 5.8 \times 10^{-6}$ M) with high absorbance at 500 nm. HABA is displaced from the HABA−avidin complex by biotin, which binds strongly to avidin ($K_d = 1 \times 10^{-15}$ M), resulting in a decrease in the absorbance of the solution at 500 nm (see Figure S5 in the Supporting Information).[56] By measurement of the change in absorbance, it is possible to quantify the amount of biotin present in solution and hence assess the effectiveness of the coupling-reaction process. The data in Table 2 show the successful reaction of the biotin at the surface of the micelles and subsequent complexation of avidin. A reference was obtained by reacting thiol-decorated particles with the HABA/avidin complex, which showed that the cross-linked micelles in solution do not interact with the HABA/avidin complex without biotin.

Our results show that 24% of the avidin was complexed to the particles, which is similar to reported values.[17] Potential explanations for this low complexation yield include (i) the possibility that some of the thiol groups at the surfaces of the micelles may not have reacted with the biotin maleimide, potentially because they are buried within the shell as a result of the molecular weight distribution of the polymeric chains and the various conformations they may adopt when assembled, and (ii) steric hindrance of the biotin in the first step and then avidin in the second step. Finally, it should be noted that the

(49) York, A. W.; Scales, C. W.; Huang, F. Q.; McCormick, C. L. *Biomacromolecules* **2007**, *8*, 2337.
(50) Wu, C. W.; Yarbrough, L. R.; Wu, F. Y. H. *Biochemistry* **1976**, *15*, 2863.
(51) Han, M. K.; Lin, P.; Paek, D.; Harvey, J. J.; Fuior, E.; Knutson, J. R. *Biochemistry* **2002**, *41*, 3468.
(52) Lindqvist, Y.; Schneider, G. *Curr. Opin. Struct. Biol.* **1996**, *6*, 798.
(53) Sakahara, H.; Saga, T. *Adv. Drug Delivery Rev.* **1999**, *37*, 89.
(54) Schetters, H. *Biomol. Eng.* **1999**, *16*, 73.
(55) Lee, H.; Kim, T. H.; Park, T. G. *J. Controlled Release* **2002**, *83*, 109.
(56) Green, N. M. A. *Biochem. J.* **1965**, *94*, 23C.

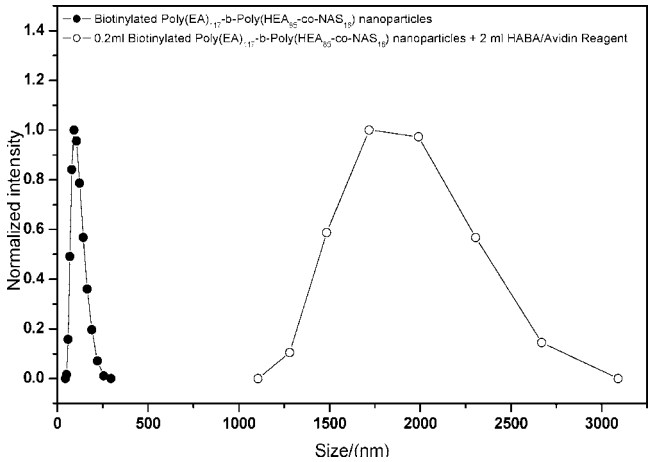

Figure 4. Particle size distribution of biotinylated SCMs from P[EA_{117}-*b*-(HEA_{85}-*co*-NAS_{16})] in water before and after conjugation to avidin.

theoretical value is most likely overestimated, as it assumes one thiol per polymeric chain, which is unlikely because of the numerous termination events occurring during radical polymerization, leading to polymeric chains without ω-functionality.

An interesting feature of the system is the use of avidin and its four subunits, each of which can conjugate one biotin molecule, as a cross-linker, resulting in the linkage of up to four different micelles together to form larger aggregates and gels. Indeed, we observed the formation of very large aggregates upon concentration of the solution containing the conjugated micelles (Figure 4). We are currently investigating the properties of these materials.

Conclusion

In summary, we have used orthogonal "relay" reactions to produce block copolymers via RAFT polymerization that can self-assemble in solution and, upon cross-linking of their shells, form soft nanoparticles. The reduction of the thiocarbonyl thio end group of the polymeric chains under mild conditions offers thiol functional groups at the surface of the nanoparticles. Thiols are an excellent handle for fast, quantitative functionalization of the particle surfaces under mild conditions, and this was exemplified by aggregation of the nanoparticles via disulfide bridges to form nanogels as well as by quantitative functionalization of the particles with a fluorescent tag or the protein avidin. This simple, rapid new route for the production of functional nanoparticles will permit a wider range of chemists to tune these materials for their own applications.

Experimental Section

Synthesis of P(EA) Macro Chain Transfer Agent (macroCTA). A stock solution containing ETSPE (0.42 g, 1.76 mmol), EA (16.65 g, 166.50 mmol), and azobis(isobutyronitrile) (AIBN) (0.03 g, 0.18 mmol) in toluene (6.5 mL) was prepared. Aliquots of this solution were placed into polymerization test tubes in a cold bath, and oxygen was removed from the solutions by bubbling with nitrogen gas for 10 min. After the solutions were degassed, the polymerization test tubes were removed from the ice bath and transferred to a heated oil bath maintained at 60 °C. Polymerization was stopped after 6 h. The resulting macroCTAs were purified by repeated dissolution of the polymer into tetrahydrofuran followed by precipitation into cold hexane. Drying of the purified macroCTAs was carried out under reduced pressure in a vacuum oven at 40 °C for 24 h, after which the polymeric CTAs were analyzed by ^{1}H NMR spectroscopy and size-exclusion chromatography.

Synthesis of P[EA-*b*-(HEA-*co*-NAS)] Polymers. P(EA) macroCTA (M_n = 11 700 g/mol, PDI = 1.1) (0.5 g) was weighed into two separate vials containing stir bars and left to dissolve in 3 mL of dry DMSO overnight. After dissolution, desired amounts of HEA and NAS were weighed into the different vials, and the contents were mixed thoroughly using a vortex mixer. AIBN (0.0020 g, 1.2 $\times$ 10^{-2} mmol) was then added to each vial from a stock solution of AIBN in DMSO, bringing the total DMSO volume to 3.5 mL. The vials were sealed using rubber septa, and the contents were thoroughly mixed and then degassed with nitrogen gas for 30 min. Polymerization was undertaken by placing the vials into a preheated oil bath at 60 °C, in which they were left for 16 h. The reactions were stopped by placing the vials into icy water. The polymers obtained were purified by repeated precipitation (three times) into cold 8:2 (v/v) hexane/diethyl ether solvent and then left to dry under vacuum. The degree of polymerization was determined by ^{1}H NMR spectroscopy using DMSO-d_6 as the solvent.

Micellization of P[EA-*b*-(HEA-*co*-NAS)] Polymers. Polymers were weighed (0.189 g) and left to dissolve in 10.5 mL aliquots of dry methanol overnight to give solutions with a concentration of 18 g/L. After polymer dissolution, the solutions were filtered through 0.2 μm membrane filters, and to the resulting solutions was added Milli-Q water (previously filtered through a 0.2 μm membrane filter) at a rate of 0.04 mL/min using an auto dispenser with constant stirring to yield solutions with a polymer concentration of 0.75 g/L.

Cross-Linking of P[EA-*b*-(HEA-*co*-NAS)] Micelles. The pH of each of the micelle solutions was first measured and then adjusted to pH 9.0−9.5 using a few drops of phosphate buffer. Known volumes of an HMDA solution prepared by dissolution of HMDA in water followed by filtration through 0.2 μm membrane filters were added to 125 mL aliquots of stirred aqueous micelle solutions at a rate of 0.1 mL/min and left to stir for 24 h. The amount of HMDA (0.0035 g/mL, 3 $\times$ 10^{-2} mmol/mL) added to each micelle solution was such that only 85% of the NAS residues were cross-linked, and the NAS/HMDA reactant ratio in solution was 2:1. An additional amount of HMDA solution equivalent to the difference between the amounts of HMDA required for 100% and 85% NAS cross-linking was added after 24 h at a rate of 0.04 mL/min, and the solution was left to stir for 4 h.

Thiol Formation on Cross-Linked Nanoparticles. Sodium borohydride solution (3 M, 25 mL, pH 10) was added to cross-linked nanoparticle solutions (90 mL), and the resulting solutions were left to stir for 16 h at room temperature. After this period, the solutions were cooled by placing them in an ice bath before neutralization by dropwise addition of hydrochloric acid with rapid stirring. After adjustment to pH 6, the solutions were brought to room temperature and left to stir for 2 h before dialysis. Dialysis was undertaken for 7 days against Milli-Q water, with the water being changed 3 times per day. After dialysis, the nanoparticle solutions (25 mL) were freeze-dried and analyzed by Raman spectroscopy.

Reaction of Thiol-Functionalized Nanoparticles with Maleimides. a. Pyrene Maleimide−Thiol Coupling. In aluminum foil-covered vials, freeze-dried cross-linked thiol-functionalized nanoparticles (~10 mg) were dissolved via sonication in 3 mL of dry DMF, after which TCEP (20 mg, 0.07 mmol), an excess relative to the theoretical number of thiol end groups on the polymer chains, was added. The vials were sealed using rubber septa, and solutions were purged with nitrogen for 2 h while stirring. *N*-1-Pyrenemaleimide solution in dry DMF (1 mL, 1 mg/mL), in excess relative to the theoretical number of thiol groups, was added, and the reaction mixtures were stirred at room temperature for 2 h under a nitrogen flow and then left for an additional 24 h at 5 °C. Milli-Q water (3 mL) was added to each sample, and the solutions were filtered through 0.45 μm membrane filters before dialysis against large volumes of Milli-Q water for 7 days in the dark at 5 °C, with

the water being changed three times per day. At the end of the dialysis period, the samples were concentrated by freeze-drying, thawed, filtered through 0.45 μm membrane filters, and refrigerated before fluorescence spectroscopy measurements. The emission spectra of the samples were obtained using fluorescence spectroscopy with the excitation wavelength set at 340 nm and a slit width of 5 nm.

b. Biotin Maleimide−Thiol Coupling. In aluminum foil-covered vials, freeze-dried cross-linked thiol-functionalized nanoparticles (∼10 mg) were dissolved in 3 mL of dry DMF, after which TCEP (20 mg, 0.07 mmol), an excess relative to the theoretical number of thiol end groups on the polymer chains, was added. The vials were sealed using rubber septa, and solutions were purged with nitrogen for 2 h while stirring. Biotin maleimide in dry DMSO (2 mL, 0.75 mg/mL), in excess relative to the theoretical number of thiol groups, was added, and reaction mixtures were stirred at room temperature for 2 h under a nitrogen flow and then left for an additional 24 h. After 24 h, 2-mercaptoethanol (0.5 mL, 7.1 mmol) was added to each of the solutions, and the solutions were left to react for 2 h at room temperature. Milli-Q water (3 mL) was added to each sample, and the solutions were filtered through 0.45 μm membrane filters before dialysis against large volumes of Milli-Q water for 7 days in the dark, with the water being changed three times per day. The samples were filtered through membrane filters (0.45 μm) and dialyzed for an additional 48 h. At the end of the dialysis period, the samples were concentrated by freeze-drying, thawed, and filtered through 0.45 μm membrane filters before UV spectroscopy measurements. Samples were analyzed using the HABA test.[51]

Acknowledgment. H.K. thanks the University of Sydney for the provision of a scholarship.

Supporting Information Available: Detailed experimental data, ^{1}H NMR spectra showing the hydrolysis of NAS and the cross-linking of micelles, TEM images of micelle solutions, Raman spectra showing the reduction of dithioester, and a UV absorption spectrum of biotinylated particles. This material is available free of charge via the Internet at http://pubs.acs.org.

JA8075499